STRESS INTENTY FACTORS FOR PLANAR CRACKS OF ARBITRARY SHAPES

Pasi Lindroth[1], Gary Marquis[1], Grzegorz Glinka[1,2]

[1] Aalto University, Helsinki, Finland

[2] University of Waterloo, Waterloo, Ontario, Canada

Abstract Fatigue crack growth models use the range and the maximum stress intensity factor to describe the driving force for crack propagation. Unfortunately, determining the stress intensity factor is not trivial, especially if the stress field and/or the crack geometry is complex. The weight function method is often used to compute stress intensity factors for cracks subjected to arbitrary loading. Weight function solutions for numerous crack geometries have been published, e.g., for through cracks, edge cracks, surface cracks and corner cracks. However, the use of the weight function for cracks of arbitrary shape is less developed.

A simplified weight function method for computing the stress intensity factor of embedded defects of arbitrary shape is discussed in this paper. The method is suitable for irregular planar cracks subjected to uniform stress distribution. The approach consists of three steps: 1) first, the crack geometry and the applied stress distribution are used to determine the average stress intensity factor around the crack perimeter, 2) secondly, the relative stress intensity factor distribution around the crack contour is computed and in step 3) the results from steps 1 and 2 are combined resulting in the determination of the actual stress intensity factor distribution along the crack perimeter. Stress intensity factor data obtained from this approach for a variety of different crack geometries are compared with available literature solutions and are found to be in good agreement.

1. INTRODUCTION

Mechanical components and engineering structures frequently contain defects that arise during manufacturing processes or are introduced in service by fatigue. In most cases they appear as material discontinuities which can be modelled as planar cracks. It is known that the size and the geometry of the initial crack have a profound effect on subsequent fatigue durability of machine components subjected to cyclic loading spectra. Estimation of safe fatigue lives of mechanical components containing flaws requires using fracture mechanics to assess fatigue crack growth. The basic parameter used in such analyses is the stress intensity factor, *K*. Therefore accurate calculation of stress intensity factors for fatigue planar cracks is essential for a reasonably accurate simulation of the fatigue crack growth and the estimation of the fatigue life of such components.

There are various methods of obtaining stress intensity factors [1, 2] discussed in the literature and numerous solutions can be found in stress intensity factor handbooks [3, 4]. However most of the available solutions have been obtained for idealized geometrical configurations such as edge, circular, elliptical and other standard crack geometries. Natural cracks are seldom circular or elliptical and therefore an efficient method of calculating stress intensity factors for planar cracks of arbitrary shapes is needed. Available analytical or numerical methods are too labour intensive and time consuming when applied for the analysis of advancing fatigue cracks. Therefore a computationally efficient approximate, but sufficiently accurate, method based on certain properties of stress intensity factors for planar cracks has been developed and validated.

2. AVERAGE STRESS INTENSITY FACTOR OVER THE CRACK FRONT OF EMBEDDED PLANAR CRACKS

With reference to Figure 1, a strong relationship has been observed between the crack surface area Λ, the length of the crack front perimeter Γ and the average stress intensity factor $\overline{K}_I$ over the entire crack perimeter where the average stress intensity factor is defined as

$$\overline{K}_I = \frac{1}{\Gamma}\oint_{\Gamma} K_I d\Gamma \quad . \tag{1}$$

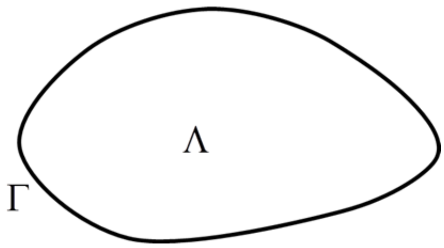

Figure 1: Crack perimeter length, Γ, and crack area, Λ, for an irregular crack

It has been also found numerically that the ratio λ of the crack area Λ to the length Γ of the crack perimeter

$$\lambda = \frac{\Lambda}{\Gamma} \tag{2}$$

is closely correlated with the average stress intensity factor $\overline{K}_I$ for any embedded convex crack subjected to uniform stress field. Based on available SIF solutions, it has been found that the following ratio is almost the same for a variety of embedded planar cracks for which the stress intensity solutions have been found in the literature, such as elliptical and square cracks [3].

$$\frac{\overline{K}_{I,A}}{\sqrt{\lambda_A}} = \frac{\overline{K}_{I,B}}{\sqrt{\lambda_B}} = \frac{\overline{K}_{I,C}}{\sqrt{\lambda_C}} = \ldots\ldots \tag{3}$$

In this equation subscripts A, B, and C indicate the average stress intensity factors, $\overline{K}_{I,A}$, $\overline{K}_{I,B}$ and $\overline{K}_{I,C}$ and ratios λ_A, λ_B and λ_C corresponding to three geometrically different embedded cracks subjected to the same uniform stress S. The validity of expression Eq. (3) has been numerically verified for a variety of circular and elliptical cracks by using Irwin's solution [5] for the elliptical crack; see Figs. 2 and 3.

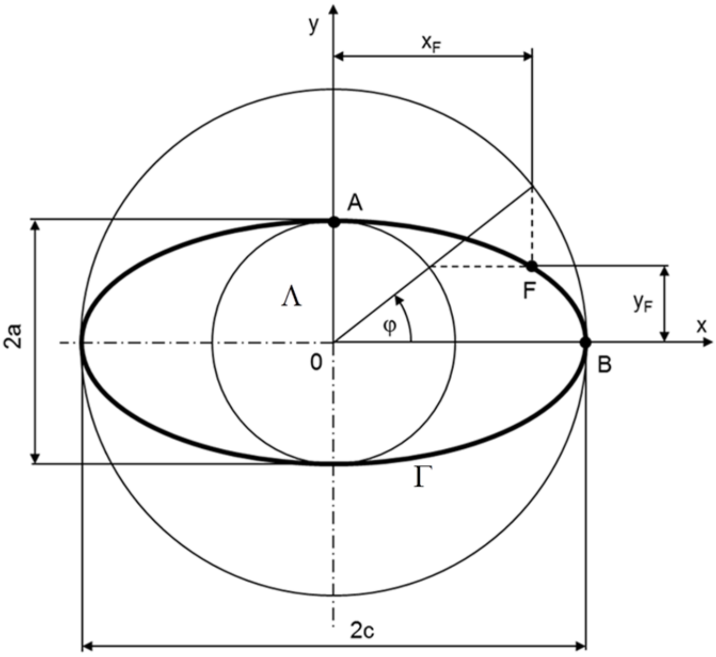

Figure 2: Parameters of an elliptical crack

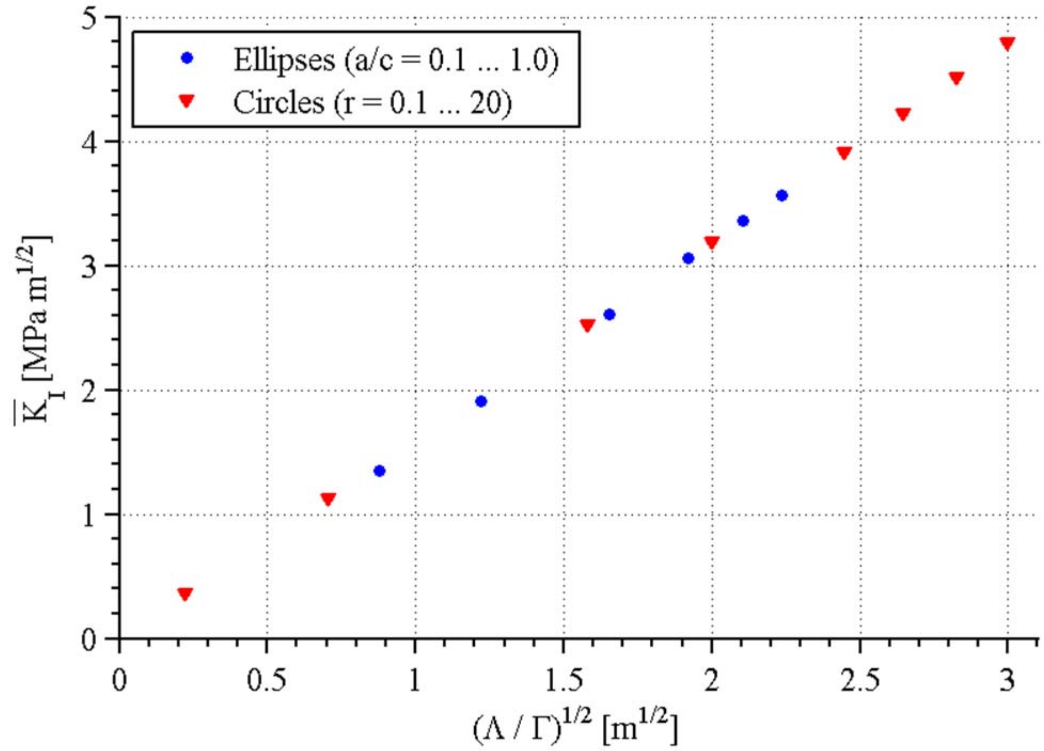

Figure 3: Relation between crack geometry and average stress intensity factor for elliptical and circular cracks.

By combing Eqs. (2) and (3), the following equation can be derived.

$$\overline{K}_{I,A}\sqrt{\frac{\Gamma_A}{\Lambda_A}} = \overline{K}_{I,B}\sqrt{\frac{\Gamma_B}{\Lambda_B}} \tag{4}$$

If it is assumed that an average geometry function for a crack, $\overline{Y}$, can be defined, the average stress intensity factor for a uniform stress field can be written as

$$\overline{K}_{I,A} = S\sqrt{\pi a_A}\overline{Y}_A;\;\; \overline{K}_{I,B} = S\sqrt{\pi a_B}\overline{Y}_B;\; etc. \tag{5}$$

Therefore, one can also write Eq. (4) as

$$S\sqrt{\pi a_A}\overline{Y}_A\sqrt{\frac{\Gamma_A}{\Lambda_A}} = S\sqrt{\pi a_B}\overline{Y}_B\sqrt{\frac{\Gamma_B}{\Lambda_B}} \tag{6}$$

and

$$\sqrt{a_A}\overline{Y}_A\sqrt{\frac{\Gamma_A}{\Lambda_A}} = \sqrt{a_B}\overline{Y}_B\sqrt{\frac{\Gamma_B}{\Lambda_B}} \; . \tag{7}$$

Because Eq. (7) was hypothesized to be valid for any convex embedded crack, it can be solved for the case of a circular crack A with radius a_A. In this case $\overline{Y}_A$ is known and Eq. (7) can be written as

$$\sqrt{a_A}\frac{2}{\pi}\sqrt{\frac{\Gamma_A}{\Lambda_A}} = \sqrt{a_B}\overline{Y}_B\sqrt{\frac{\Gamma_B}{\Lambda_B}} \; . \tag{8}$$

Therefore, the average geometrical factor $\bar{Y}_B$ can be written as

$$\begin{aligned} \sqrt{a_A}\,\frac{2}{\pi}\sqrt{\frac{2\pi a_A}{\pi a_A^2}} &= \sqrt{a_B}\,\bar{Y}_B\sqrt{\frac{\Gamma_B}{\Lambda_B}} \\ \bar{Y}_B &= \frac{2\sqrt{2}}{\pi}\sqrt{\frac{\Lambda_B}{a_B\Gamma_B}} \end{aligned} \tag{9}$$

Equation 9 shows that the average geometric factor $\bar{Y}$ for any embedded crack can be written in terms of the characteristic crack size a, the crack surface area Λ and the length of the perimeter Γ.

$$\bar{Y} = \frac{2\sqrt{2}}{\pi}\sqrt{\frac{\Lambda}{a\cdot\Gamma}} \tag{10}$$

The average stress intensity factor $\bar{K}_I$ for any embedded crack can be subsequently calculated from

$$\bar{K}_I = S\sqrt{\pi a}\,\bar{Y} = S\sqrt{\pi a}\,\frac{2\sqrt{2}}{\pi}\sqrt{\frac{\Lambda}{a\cdot\Gamma}} \tag{11}$$

It can be noted that the characteristic crack size a cancels out and, after some simplification, the average stress intensity factor for an embedded crack takes the form:

$$\bar{K}_I = 2S\sqrt{\frac{2\Lambda}{\pi\Gamma}} \tag{12}$$

3. VARIATION OF THE STRESS INTENSITY FACTOR ALONG THE CRACK FRONT

The variation of the stress intensity factor along the crack front has been approximated by assuming that the crack front points are affected only by the stress field in an area Ω which is can be considered as neighbouring the point of interest on the crack front. The shape and size of Ω are varies at each point along the crack front and depends on the local geometry of the crack contour. The assumption is that only that portion of the contour which is closest to the point of interest carries the load and shielding the rest of the crack contour. For the arbitrary point $A(x_A, y_A)$ along an irregular planar crack front, Ω_A is defined as shown in Fig. 4.

$$\Omega_A = \left\{ P(x,y) \in \Lambda \,\middle|\, d(x,y,x_A,y_A) \le \alpha s(x,y,\Gamma) \right\} \tag{13}$$

With reference to Fig. 4, $P(x, y)$ is an arbitrary point inside the crack, Λ is the crack area, $d(x, y, x_A, y_A)$ is the distance between points $P(x, y)$ and $A(x_A, y_A)$, $s(x, y, \Gamma)$ is the shortest distance between point $P(x, y)$ and the crack contour Γ and α is a parameter used to define the size of Ω_A.

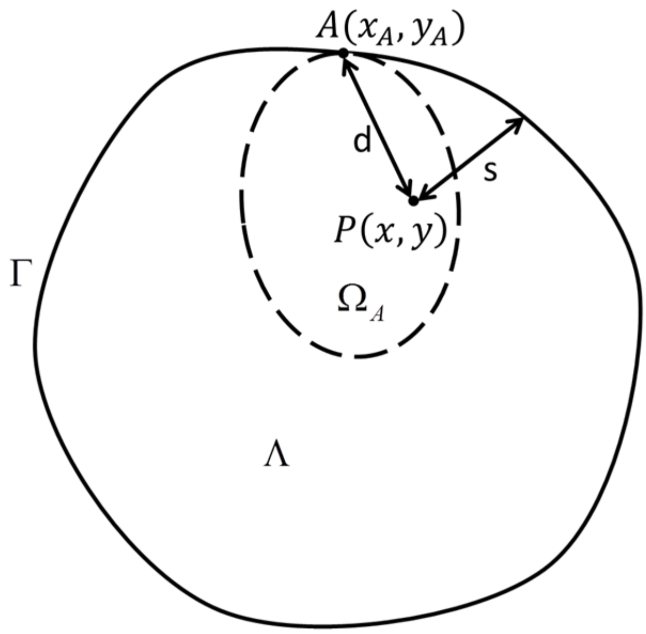

Figure 4: Area contributing to stress intensity factor at point A.

The upper limit of α has been derived from the stress intensity factor solution of a square crack. The zero stress intensity factors at the corners of the square crack are obtained only by using the values less than $\sqrt{2}$. Therefore the value of the factor α must be between 1.0 and $\sqrt{2}$.

The force that contributes to the point A can be calculated as

$$F_A = \oint_{\Omega_A} \sigma(x, y) dx dy \quad . \tag{14}$$

The force distribution, *F*, is obtained when Eq. (14) is calculated at the each point along the crack front. It has been found that the stress intensity factor distribution is approximately proportional to the force distribution

$$k_I \approx \beta F^{1/4} \tag{15}$$

where β = constant.

This distribution defines the variation of the stress intensity factor along the crack perimeter. The actual stress intensity factor distribution has been obtained by using the average stress intensity factor and the relative stress intensity factor distribution.

$$K_I = k_I \frac{\overline{K}_I}{\overline{k}_I} \tag{16}$$

where K_I is the actual stress intensity factor distribution, $\overline{K}_I$ is the average stress intensity factor from Eq. (12) and $\overline{k}_I$ is the average relative stress intensity factor calculated as

$$\overline{k}_I = \frac{1}{\Gamma} \oint_{\Gamma} k_I d\Gamma \approx \frac{\beta}{\Gamma} \oint_{\Gamma} F^{1/4} d\Gamma \quad . \tag{17}$$

4. NUMERICAL IMPLEMENTATION

The force distribution *F* has been calculated numerically and therefore the crack geometry and the stress field over the crack area have to be discrete. The crack geometry has been discretized by using linear segments and the stress intensity factors have been calculated in the middle of the segments. The continuous stress field has been discretized by dividing the crack area into smaller areas and the stress fields over these areas have been replaced by discrete forces.

The force contributing to the i^{th} stress intensity factor point has been calculated as

$$F_i = \sum_{j=1}^{n} \begin{cases} P_j & ,d_j < \alpha s_j \\ 0 & ,d_j \geq \alpha s_j \end{cases} \quad . \tag{18}$$

Where P_j is the discrete force, d_j is the distance between P_j and the i^{th} stress intensity factor point, s_j is the shortest distance between P_j and the crack contour, and n is the number of the discrete forces.

The discrete relative stress intensity factor distribution is obtained from F_i as

$$k_{I,i} = \beta F_i^{1/4} \quad . \tag{19}$$

The actual stress intensity factor at the i^{th} stress intensity factor point is

$$K_{I,i} = k_{I,i} \frac{\overline{K}_I}{\overline{k}_I} \quad . \tag{20}$$

Where $\overline{K}_I$ is the average stress intensity factor from Eq. (12) and $\overline{k}_I$ is the average relative stress intensity factor calculated as

$$\overline{k}_I = \frac{1}{n} \sum_{i=1}^{n} k_{I,i} = \frac{\beta}{n} \sum_{i=1}^{n} F_i^{1/4} \quad . \tag{21}$$

5. RESULTS

Stress intensity factor data obtained from Eq. (21) for a variety of different crack geometries has been compared with available literature solutions. The crack geometry was discretized by using 200 linear segments but the number of the discrete forces was varying between different crack geometries. However, the number of discrete forces was large in each case so as to improve agreement between the numerical implementation and the actual integral equation. The value of $\alpha = 1.4$ was used in all cases.

5.1. Square Crack

The SIF for a square crack has been compared to published handbook solution obtained using the finite element method [3], see Fig. 5. The length of the side is 2a. Error at the most critical point is 2.3%. The zero stress intensity factor was obtained at $s/a = 1$ because α was less than $\sqrt{2}$.

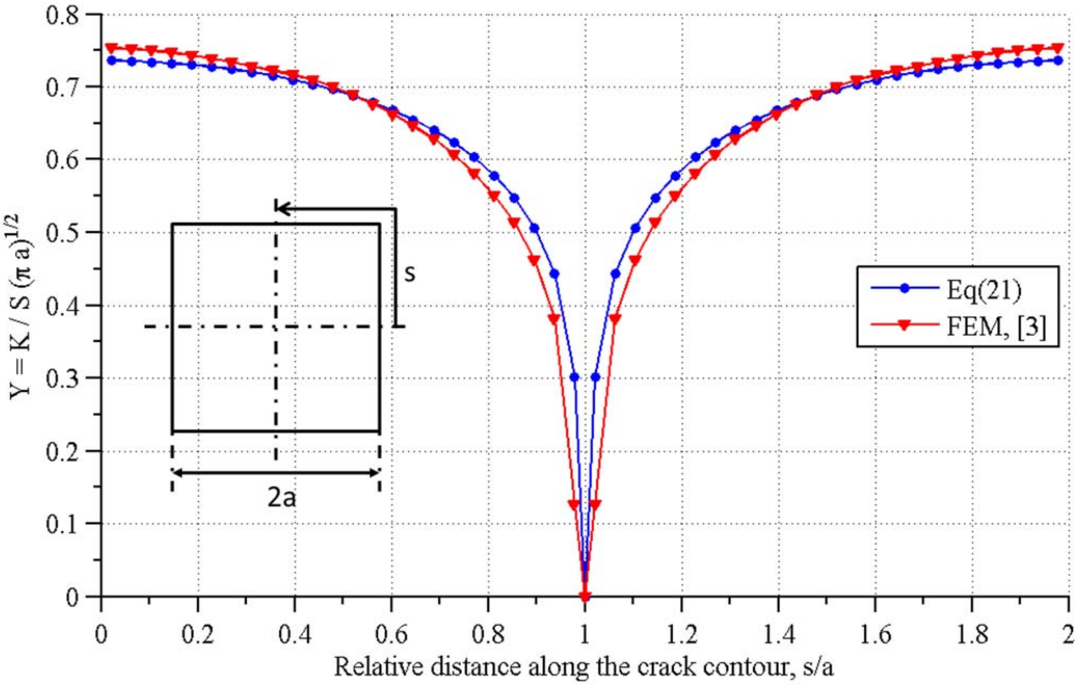

Figure 5: Reference and Eq. (21) based SIFs for a square crack. Parameter s is the length along the crack contour starting from middle of one side.

5.2. Half elliptical - half circular Crack

A non-standard crack created by joining half a circle and half an ellipse was also analyzed, see Fig. 6. The SIF for the half elliptical – half circular crack based on Eq. (21) is compared to the analytical data of Mastrojannis et al [6], see Fig. 6. The c/a ratio of the ellipse is 1.5 and the radius of the circle is a. The difference in SIF at the point of greatest SIF is less than 1.3%.

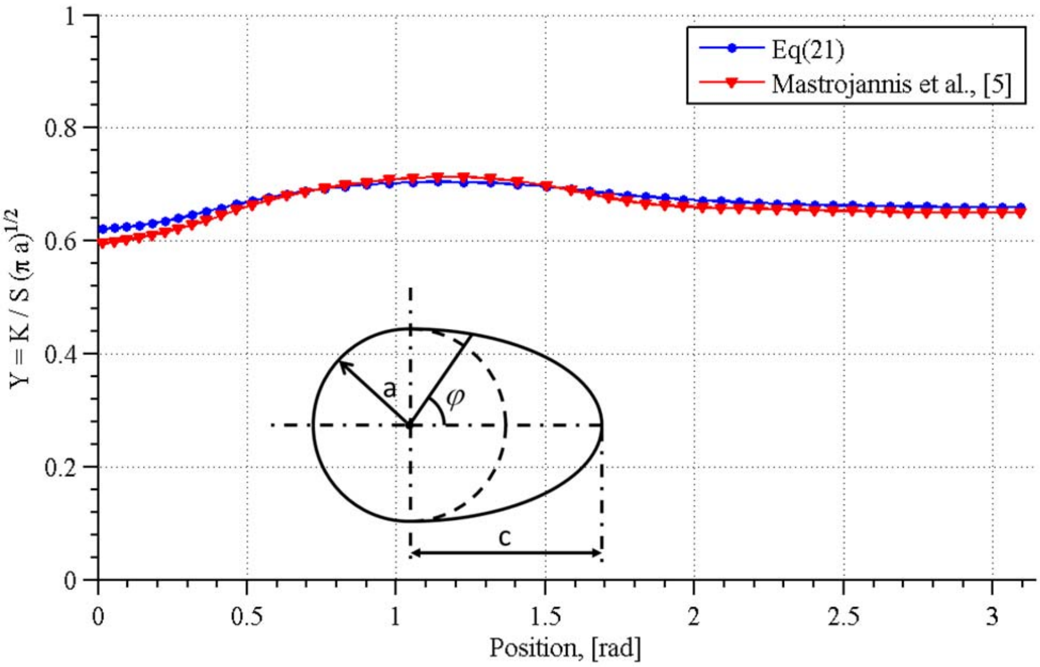

Figure 6: Reference and Eq. (21) based SIFs for a half elliptical - half circular crack

5.3. Elliptical Crack

The stress intensity factors from elliptical cracks with different a/c ratio have been compared to Irwin's solution [5], see Fig. 7. Error at the most critical point, $\varphi = {}^{\pi}/_{2}$, is less than 4.5% for ${}^{a}/_{c} = 0.01$ and less than 3% for ${}^{a}/_{c} = 0.1$. Ellipses with small a/c ratio require that the stress field discretization is dense enough. Rough discretization will cause zero stress intensity factors at the ends of the major axis.

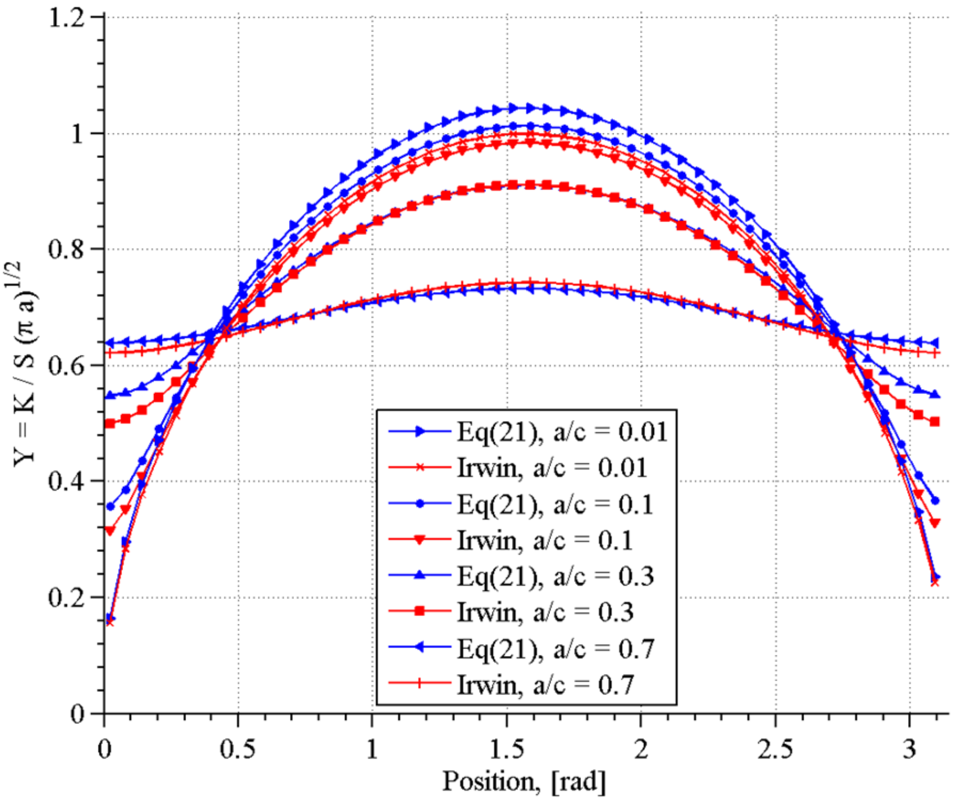

Figure 7: Reference and Eq. (21) based SIFs for two elliptical cracks with different a/c ratios

6. CONCLUSION

A strong relationship between the surface area of the crack, length of the crack perimeter and the average stress intensity factor over the entire crack perimeter has been found for a variety of embedded convex planar cracks of different shapes. The average stress intensity factor can be used to estimate the stress intensity factor distribution along the crack line if relative distribution is known. Therefore the new method to approximate the relative stress intensity factor distribution has been developed.

The results from the new method have been compared to the stress intensity factor solutions from literature for several crack shapes: elliptical cracks, a square crack and a half ellipse – half circle crack. In all comparisons the difference is less than 4.5%.

7. References

1. M.H. Aliabadi and D.P. Rooke, Numerical Fracture Mechanics, Computational Mechanics Publications, Southampton, 1990.

2. T.L. Anderson, Fracture Mechanics-Fundamentals and Applications, CRC Press, Boca Raton, 1995.

3. Y. Murakami et. al, (editor), Stress Intensity Factors Handbook, Pergamon Press, Oxford, 1987.

4. H. Tada, P. Paris and G. Irwin, The Stress Analysis of Cracks Handbook. 2nd ed., Paris Production Inc., St. Louis, 1985.

5. W.F. Brown and J.E. Srawley, Plane Strain Crack Toughness Testing of High Strength Metallic Material, ASTM STP 410, American Society for Testing and Materials, Philadelphia, 1966, 110 – 114.

6. E.N. Mastrojannis, L.M. Keer and T. Mura, *International Journal of Fracture*, 15 (3), 1979.